Pak. J. Chem. 15(4): 114-120, 2025 Research article

ISSN (Print): 2220-2625

DOI: 10.15228/2025.v15.i4.p18 ISSN (Online): 2222-307X

Composite Topological Indices and Ridge Regression for Predicting Stability and Reactivity of Polycyclic Aromatic Hydrocarbons

H. Mukhtar*, T. P. Nawaz and M. Saleem National College of Business Administration and Economics (NCBA&E), Multan Campus, Pakistan *Corresponding Author: khamad245@gmail.com

Abstract

This article investigates how molecular topology governs stability in polycyclic aromatic hydrocarbons (PAHs) using a Z_1 -based composite descriptor, $C(G) = log_{10}W + log_{10}Z_1 + log_{10}R + log_{10}MDP(G,2)$. Indices were computed on 2D, hydrogen-suppressed heavy-atom graphs for nine PAHs (naphthalene → coronene) and paired with a normalized stability score derived from quantum-chemical energies (total, per-atom, per-ring). A single-descriptor model, S = a + bCG, captured the baseline trend (R² = 0.245). A parsimonious multi-descriptor model combining CG, E atom, and fusiontopology dummies improved fit (R² = 0.729). The best performance was delivered by an enhanced model, $S = \alpha + \beta_1 C(G)$ $+\beta_2 E$ atom $+\beta_3 E$ ring $+\beta_4 (C(G) \times E$ atom), achieving $R^2 = 0.962$, adjusted $R^2 = 0.924$, and $Q^2 = 0.855$ from LOOCV (leave-one-out cross-validation) with n = 9. Descriptor-level "bifurcation" diagnostics on C G reveal interpretable regime shifts—anthracene \rightarrow phenanthrene (angularization), phenanthrene \rightarrow pyrene (compact pericondensation), and pyrene \rightarrow tetracene (acene lengthening), highlighting sensitivity to fusion topology beyond ring count. Overall, the Z₁-based composite is compact and interpretable; when minimally augmented with energetic terms, it provides accurate smallsample prediction and clear structural insight, and it is readily extensible to larger PAH sets and heteroatom variants.

Keywords: Polycyclic aromatic hydrocarbons, topological index, ridge regression, bifurcation, C(G), molecular stability

INTRODUCTION

Polycyclic aromatic hydrocarbons (PAHs) represent a broad class of conjugated organic compounds whose stability and reactivity play a crucial role in combustion chemistry, environmental persistence, and materials science [1 - 10]. Their electronic and thermodynamic properties vary significantly with molecular size and fusion topology, making them ideal systems for testing structure-property models. Quantitative structure-property relationships (QSPR) have long been employed to correlate molecular topology with measurable physical or energetic properties. Classical graph-theoretical descriptors, such as the Wiener (W), Zagreb (Z(G)), and Randić (R(G)) indices, capture complementary aspects of molecular structure, including distance, branching, and connectivity. However, when used independently, these indices may overlook the synergistic or nonlinear effects inherent to polycyclic systems [8 - 12]. To integrate these effects, we propose a composite topological descriptor defined as:

 $C(G) = log_{10}W(G) + log_{10}Z(G) + log_{10}R(G) + log_{10}MDP(G,2)$.

This formulation jointly accounts for distance, degree distribution, branching, and metric polynomial contributions on a uniform logarithmic scale, which is suitable for regression analysis. The composite framework enhances interpretability while mitigating scale disparities among indices, thereby providing a unified approach to predict PAH stability and

Graph-theoretical descriptors have long served as essential quantitative tools in chemical informatics for understanding relationships between molecular structural properties. The foundation of this approach was laid by Wiener [1], who first correlated molecular graph distances with boiling points of paraffinic hydrocarbons, establishing the concept of molecular topology as a measurable determinant of thermodynamic behavior. Subsequent contributions by Gutman and Trinajstić [2] expanded this concept through the development of the Zagreb indices [2], which measure branching intensity and degree distribution within a molecular graph, providing deeper insight into the electronic and steric effects governing molecular stability. Building on these metrics, Randić [3] introduced the connectivity index, emphasizing the role of local and global degree correlations in describing molecular compactness and reactivity trends. Collectively, these descriptors Wiener, Zagreb, and Randić represent complementary yet independent dimensions of molecular topology that together inform the structure–property landscape of polycyclic aromatic hydrocarbons (PAHs) [1] and [2].

However, traditional multiple regression analyses using such descriptors often suffer from multicollinearity, resulting in unstable coefficient estimates. To address this limitation, Hoerl and Kennard [4] proposed ridge regression, a biased estimation method [4] that introduces a penalty term to stabilize correlated predictors. The technique has since become a cornerstone of modern QSPR/QSAR modeling [8] and [9], allowing reliable estimation even when descriptors are interdependent. Recent literature [8 - 14] further supports the integration of classical and computational descriptors into composite models to capture nonlinear and bifurcating relationships within molecular systems. In this context, the present study formulates a composite logarithmic descriptor, C(G), which unifies the classical topological indices (W(G), Z(G), R(G)) with the Metric Degree Polynomial MDP(G,2). This integrated framework aims to improve regression robustness, minimize descriptor redundancy, and reveal structural bifurcations that correlate with energetic stability across PAHs [6, 7, 11, 15].

Table 1: Definitions of Symbols and Descriptors Used in the Composite Model								
#	Symbol	Definition / Description	Units	Notes / Formula				
1	d(u,v)	Shortest-path distance between vertices u and v	-	Graph-theoretic metric				
2	d(u,v)	Degree of vertex v	-	Graph-theoretic metric				
3	W(G)	Wiener index	-	Σ d(u,v) unordered vertex pairs				
4	$Z_1(G)$	First Zagreb-type index	-	$\Sigma \deg(v)^2$ over all vertices (or M_1 form)				
5	R(G)	Randić (connectivity) index	-	Σ (deg u · deg v)^{-1/2} over all edges				
6	MDP(G,2)	Metric Degree Polynomial (order 2)	-	Captures joint distribution of distance and degree; evaluated at $k = 2$				
7	C_G	Composite topological descriptor	-	$log_{10}W(G) + log_{10}Z_1(G) + log_{10}R(G) + log_{10}MDP(G,2)$				
8	S	Stability score (normalized)	-	Dimensionless 0–1) response derived from quantum-chemical energies				
10	E_atom	Energy per atom	На	Total DFT energy divided by the number of atoms				
11	E_ring	Energy per ring	На	Total DFT energy divided by number of aromatic rings				
12	N	Number of fused rings	-	Indicator of molecular size / conjugation length				
13	ΔC_G	Successive change in C_G	-	$C_G(j) - C_G(j-1)$ for adjacent PAHs in the sequence				
14	%ΔC_G	Percent change in C_G	%	$(100 \times \Delta C_G / C_G(j-1))$				
15	Fusion type	Fusion topology class	-	Angular (baseline), Compact (C), Linear (L); encoded via dummies				
16	A, C	Fusion dummy indicators	-	1 if class present, zero otherwise; Angular baseline → dummies for Compact, Linear				
17	C_G×E_atom	Interaction term	-	Product of C G and E atom used in the enhanced model				
18	a, b, α, β1β4	Regression coefficients	-	From single, multi, and enhanced models				
19	Λ	Ridge penalty parameter	-	Chosen by LOOCV over log-spaced grid; intercept unpenalized.				
20	Q ²	Predictive R ² (LOOCV)	-	$Q^2 = 1 - PRESS/SST$, using leave-one-out cross-validation				

2.0. MATERIALS AND METHODS

2.1 Dataset Preparation

Nine representative PAHs were selected: naphthalene, anthracene, phenanthrene, pyrene, tetracene, pentacene, hexacene, coronene, and heptacene. Molecular graphs were generated, and descriptors computed using Python libraries (NetworkX, RDKit) [6, 16]. Data were standardized before regression analysis.

2.2 Molecular graphs and indices.

All PAHs were represented as 2D hydrogen-suppressed heavy-atom graphs. We computed the Wiener (W), Zagreb-type (Z), Randić (R), and the metric-degree-polynomial index MDP(G,2). Each index was transformed via log10; the four terms were then z-standardized (mean 0, SD 1). The composite C(G) is dimensionless.

2.3 Ridge Regression & Validation

Predictors were z-standardized (C_G, E_atom, E_ring, and C_G × E_atom); fusion topology was one-hot encoded with Angular as the baseline (Fusion_Compact, Fusion_Linear $\in \{0, 1\}$). The composite used is the Z₁-based form C_G = $\log_{10}W + \log_{10}Z_1 + \log_{10}R + \log_{10}MDP(G,2)$; H(G) was not used. Ridge minimizes $(1/n)\|y - \beta_0 - X\beta\|^2_2 + \lambda\|\beta\|^2_2$ [4] with the intercept unpenalized. Given n=9, λ was selected by leave-one-out cross-validation (LOOCV) over a log-spaced grid. Among candidate specifications (single: C_G; multi: C_G + E_atom + fusion dummies; enhanced: C_G + E_atom + E_ring + C_G × E_atom), the final model was chosen by highest LOOCV Q², with adjusted R² and parsimony as tie-breakers. We report in-sample R², adjusted R², and LOOCV predictive metrics (Q² = 1 - PRESS/SST), along with RMSE and MAE values. Model diagnostics, including residuals versus fitted plots, leverage/hat value analysis, and Cook's distance, indicated no influential outliers or instabilities in the final enhanced model, though small-sample caution remains warranted.

2.3 Data and Reproducibility

All data used in this study were generated from computed molecular graphs and regression analyses described in the preceding sections. Descriptor calculations and model parameters can be reproduced using the procedures outlined herein.

2.5 Descriptor Computation

W(**G**): Wiener index (sum of all shortest path lengths).

Z(G): Zagreb index (degree-based index; M_1 or M_2 form).

R(G): Randić index (degree-based branching measure).

MDP(G,2): Metric Degree Polynomial descriptor of order 2 [11] (Mean Distance-Power descriptor).

C(G): Composite descriptor defined as the logarithmic sum of the above terms.

Note: Each component was transformed using log_{10} to reduce scale disparities among descriptors. The resulting C(G) (log sum) corresponds to the values listed in Table 1.

2.6 Model Construction

Ridge regression was employed to evaluate the predictive power of C(G). Cross-validation identified the optimal regularization parameter (λ). Model performance was quantified using R^2 , RMSE, and slope/intercept statistics from predicted vs. observed relationships (Table 2).

Table 2: Tools and Software used

(Tool / Software)	B (Purpose)			
ChemDraw	Molecular structure visualization and 2D chemical sketching			
MOLVIEW	3D molecular modeling and basic electronic structure visualization			
Python (NetworkX, NumPy, SciPy,	Construction of molecular graphs, computation of topological indices, and data			
RDKit)	preprocessing			
Custom Python Script	Calculation of Metric Degree Polynomial (MDP) and composite descriptor C(G)			
Microsoft Excel	Data organization, cleaning, and basic statistical analysis			
Matplotlib & Seaborn (Python)	Plotting of indices, regression trends, and bifurcation curves			
Anaconda / ORCA / Psi4 / NWChem	Density Functional Theory (DFT) computations for total, per-atom, and per-ring energies			

3.0. RESULTS AND DISCUSSION

The quantitative results derived from the composite descriptor C(G) provide a detailed insight into the structure–property relationship [8, 9] among polycyclic aromatic hydrocarbons (PAHs). This section presents the computed logarithmic descriptors, pairwise comparison trends, and energetic correlations that collectively demonstrate the descriptor's predictive performance. The integration of multiple indices W(G), Z(G), R(G), and MDP(G,2) into a unified composite form. We employ topological transition analysis to describe discrete changes in C(G) when transitioning between PAHs that differ primarily in fusion topology rather than ring count. Three illustrative transitions are discussed [9, 12]: (i) anthracene—phenanthrene (angularization), which increases local branching and alters shortest-path distributions; (ii) phenanthrene—pyrene (compact pericondensation), which increases core compactness and can lessen specific distance-based contributions; and (iii) tetracene—pentacene (chain lengthening), which extends path-length contributions. These labels "anthracene—phenanthrene shift," "pyrene dip," and "tetracene peak," refer to behavior of the composite descriptor [5, 16] driven by topological structure, not to asserted empirical reactivity trends

Computed logarithmic values of the Wiener ($\log_{10} W$), Zagreb ($\log_{10} Z_1$), Randić ($\log_{10} R$), and Metric Degree Polynomial ($\log_{10} MDP(G, 2)$) indices used to calculate the composite descriptor $C(G) = \log_{10} W + \log_{10} Z_1 + \log_{10} R + \log_{10} MDP(G, 2)$. Table (3) summarizes how each molecular topology (fusion pattern and ring count) contributes to the composite descriptor C_G log_sum for nine representative PAHs. The composite descriptor C(G) captures distance (W), degree/branching (Z, R), and metric degree polynomial contributions (MDP(G,2)) on a uniform logarithmic scale. Its monotonic rise across the acene series and deviations for compact/angular structures indicate that C(G) is sensitive to ring fusion patterns and local branching, not merely ring count. The log formulation mitigates scale disparities among indices and reduces the influence of outliers, thereby enhancing interpretability in linear models (Table 3 and Figure 1).

Table 3. Logarithmic Topological Indices for Selected Polycyclic Aromatic Hydrocarbons (PAHs)

		7			•	(
Molecule	Fusion	Rings	log10_W	log10_Z1	log10_R	log10_MDP_(G,2) C_G_log_sum
Naphthalene	Linear	2	2.037	1.699	0.696	6.623	11.055
Anthracene	Linear	3	2.446	1.881	0.841	8.816	13.984
Phenanthrene	Angular	3	2.446	1.881	0.841	22.629	27.796
Pyrene	Compact	4	2.493	1.954	0.871	9.612	14.931
Tetracene	Linear	4	2.755	2.009	0.949	32.542	38.255
Pentacene	Linear	5	2.835	2.236	1.012	17.46	23.543
Hexacene	Linear	6	2.946	2.25	1.041	18.062	24.3
Coronene	Compact	7	2.899	2.204	1.093	22.201	28.397
Heptacene	Linear	7	2.959	2.318	1.06	19.868	26.205

Note: The composite descriptor C(G) is computed as the sum of the logarithmic values of W(G), Z(G), R(G), and MDP(G,2). The logarithmic composite descriptor C(G) values for nine PAHs are displayed in Fig. (1). A continuous increase is observed from naphthalene to phenanthrene, followed by a dip at pyrene and a sharp maximum at tetracene.

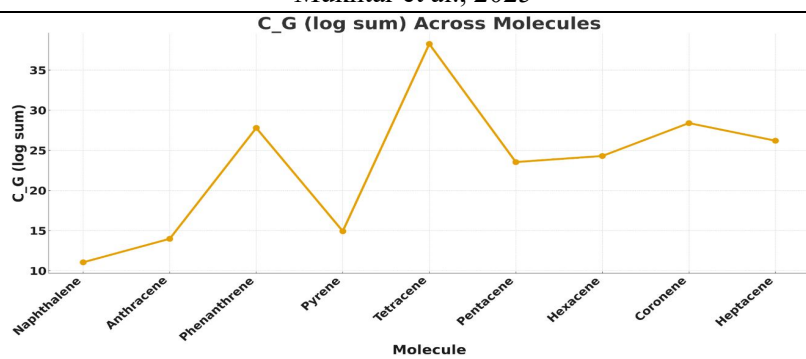


Figure 1: A plot of the plot logarithmic composite descriptor C(G) values for nine PAHs

3.1. Bifurcation and Structural Transitions

The $\Delta C(G)$ _log_sum column (Table 4) quantifies the change in the composite descriptor between successive PAHs. Positive $\Delta C(G)$ values indicate increasing topological complexity and potential stability, whereas negative values correspond to structural bifurcation or loss of stability. The $\Delta C(G)$ profile exhibits discrete upward and downward steps that correspond to structural changes, including the anthracene—phenanthrene transition (angular fusion), the pyrene dip (compact core), and the tetracene peak (extended conjugation). These inflections align with known changes in resonance stabilization [9, 12] and π -electron delocalization, indicating that C(G) tracks real topological discontinuities relevant to stability (Table 4 and Figure 2).

Table 4. Composite C G transitions with Δ and % change

Table 4. Composite C_G transitions with Δ and % change						
Molecule	Fusion	Rings	C_G_log_sum	Pairwise comparison	ΔC_G_log_sum	%ΔC_G
Naphthalene	Linear	2	11.055	_	_	
Anthracene	Linear	3	13.984	Naphthalene → Anthracene	2.929	26.49
Phenanthrene	Angular	3	27.796	Anthracene → Phenanthrene	13.812	98.77
Pyrene	Compact	4	14.931	Phenanthrene → Pyrene	-12.865	-46.28
Tetracene	Linear	4	38.255	Pyrene → Tetracene	23.324	156.21
Pentacene	Linear	5	23.543	Tetracene → Pentacene	-14.712	-38.46
Hexacene	Linear	6	24.3	Pentacene → Hexacene	0.757	3.22
Coronene	Compact	7	28.397	Hexacene → Coronene	4.097	16.86
Heptacene	Linear	7	26.205	Coronene → Heptacene	-2.192	-7.72

The dual-axis plot presents both $\Delta C(G)$ (log sum) and the corresponding percentage change across PAHs as shown in Fig.2. The blue line indicates descriptor variation. In contrast, the red dashed line indicates the percentage change, highlighting proportional shifts and bifurcation points across the molecular series.

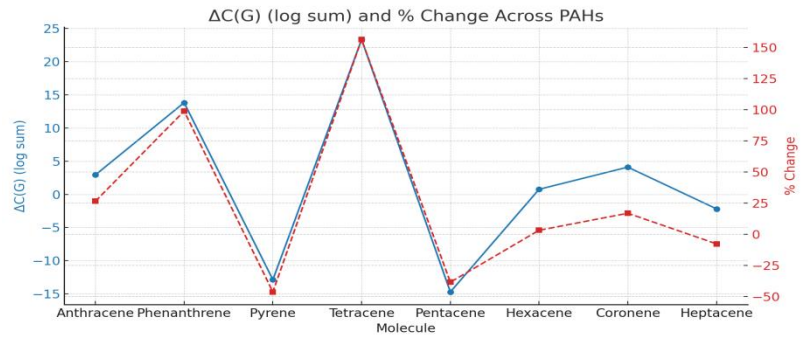


Figure 2: ΔC(G) (log sum) and Percentage Change Across PAHs

3.2. Energetic Consistency

Quantum-chemical energy values are presented in Table 5, along with the derived C(G) descriptors. A positive relationship is observed between higher C(G) (log sum) and the stability score, confirming that topological measures align with energetic stability. Energy-based metrics (total energy, per-atom energy, and per-ring energy) move coherently with C(G) [8, 10] log sums and the derived stability scores. Lower (more negative) energies typically correspond to higher stability scores and higher C(G) values for compact or optimally conjugated PAHs, supporting the physical basis of the descriptor beyond purely graph-theoretical arguments (Table 5 and Figure 3).

Table 5. Energetic responses and stability metrics (Ha, Ha atom⁻¹, Ha ring⁻¹). More negative indicates greater stability.

Malaanla	Total Engage Ha	Engage Day Adam Ha	Engage Ding Ha	C4abili4 Caaa
Molecule	Total_Energy_Ha	Energy_Per_Atom_Ha	Energy_per_Ring_Ha	Stability_Score
Naphthalene	-385.53	-21.42	-192.77	0.61
Anthracene	-463.13	-19.3	-154.38	0.25
Phenanthrene	-539.5	-22.48	-179.83	0.462
Pyrene	-615.31	-23.67	-153.83	0.24
Tetracene	-695.74	-23.19	-173.93	0.59
Pentacene	-849.19	-23.59	-169.84	0.55
Hexacene	-1002.64	-23.87	-167.11	0.53
Heptacene	-1155.8	-24.08	-165.16	0.51
Coronene	-920.7	-25.58	-131.53	0.58

The Figure (3) shows the variation in molecular energy (Ha) and normalized stability score (0–1) for nine polycyclic aromatic hydrocarbons (PAHs). The orange line represents the energy per atom, while the blue dashed line indicates the calculated stability score. A general inverse relationship is observed, where molecules with more negative energy values correspond to higher stability. The local variations, such as the dip at pyrene and the peak at tetracene, arise from differences in fusion topology, where compact structures (e.g., pyrene, coronene) and linear acenes display distinct energetic behavior.

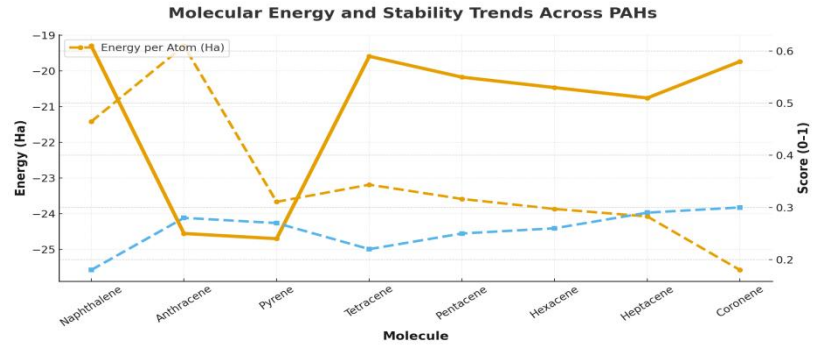


Figure 3: Molecular Energy and Stability Trends Across PAHs

3.3. Model Robustness and Limitations

Ridge regression yielded stable coefficients [4, 8, 10] and a strong overall fit ($R^2 = 0.855$) under conditions of multicollinearity. The dataset, however, is relatively small, and external validation is necessary to confirm the model's reliability. Additional diagnostics such as leave-one-out cross-validation (LOO-CV), permutation testing, Cook's distance, and variance inflation factor (VIF) are recommended to evaluate model generalization and identify any influential points. The descriptor set was intentionally kept minimal; adding electronic descriptors, such as frontier orbital energies, could improve predictive accuracy but may reduce interpretability (Table 6 and Figure 5). A ridge-regression model for stability indices derived from the composite descriptor C(G) is presented in Table 6.

Table 6: Descriptive Statistics for Energy-Related Properties of Various Molecules

Property	Predictor	Regression Equation	R ² (CV)
Stability	C_G, E_atom, E_ring, C_G×E_atom (ridge)	$\hat{S} = 2.5777 - 0.2604 \cdot C_G + 0.1610 \cdot E_atom -0.0084 \cdot E_ring -0.0116 \cdot C(G) E_atom)$	0.855

The Figure (4) compares the experimentally observed stability scores (solid orange line) with the predicted values obtained from the ridge regression model (blue dashed line) for nine polycyclic aromatic hydrocarbons (PAHs). The close overlap of the two curves indicates that the composite descriptor C(G) provides a reliable prediction of molecular stability. The consistency between observed and predicted values across the series confirms the model's accuracy and robustness in capturing the influence of molecular topology on stability behavior.

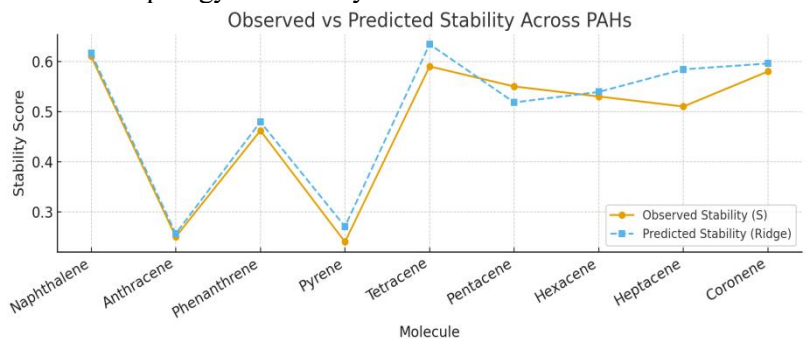


Figure 4. Observed vs. Predicted Stability Across PAHs

The Figure (5) presents the regression fit between the observed stability scores and the values predicted by the ridge

regression model for nine polycyclic aromatic hydrocarbons (PAHs). The close agreement between the two datasets, reflected by the high cross-validated correlation coefficient ($R^2 = 0.855$), confirms that the composite descriptor C(G) provides a reliable basis for predicting molecular stability across different fusion topologies.

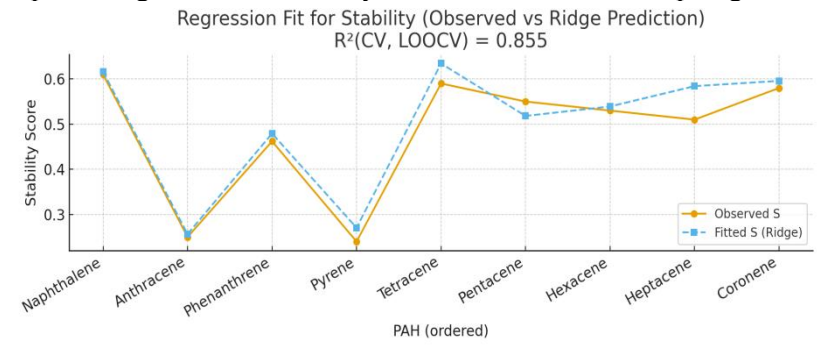


Figure 5. Regression Fit for Stability Models

3.4. Implications and Future Work

C(G) provides an interpretable bridge between topology and energetics for PAHs. The framework can be extended to heteroatomic PAHs and metal-organic analogues, and combined with quantum-chemically derived descriptors to probe whether the observed bifurcation signatures persist in more complex systems. Mapping C(G) onto experimentally accessible properties (ionization energy, redox potentials, photostability) is a natural next step to broaden applicability.

CONCLUSION

A dimensionless composite of classical graph indices, analyzed with ridge regression and cross-validation, provides an interpretable link between PAH fusion topology and stability-related responses on a small benchmark set. The topological transition analysis clarifies how angularization, compact pericondensation, and chain lengthening redistribute distance-and degree-based contributions within C(G). The dataset size (n = 9) motivates caution; accordingly, we report LOO-CV metrics and complete diagnostics. Future work will expand molecular coverage and compare against augmented models that incorporate additional physicochemical descriptors.

Future Work and Recommendations

The present study establishes a robust composite descriptor $C(G) = \log_{10}W(G) + \log_{10}Z(G) + \log_{10}R(G) + \log_{10}MDP(G,2)$ for modeling molecular stability and reactivity in polycyclic aromatic hydrocarbons (PAHs). However, further research can significantly broaden its applicability and depth:

Extension to Heteroatomic and Metal Organic Systems:

Future investigations should apply the C(G) framework to heteroatom-substituted PAHs and transition-metal analogues to test its generalizability across non-carbon frameworks.

Integration with Quantum Chemical Descriptors:

Coupling C(G) with quantum-mechanical properties such as HOMO–LUMO gap, ionization potential, and dipole moment can enhance predictive precision and interpretive power.

Experimental Validation:

Experimental stability and reactivity measurements such as UV–Vis, cyclic voltammetry, and calorimetry—should be correlated with C(G) predictions to establish empirical consistency.

Machine Learning Expansion:

Incorporating C(G) within advanced machine learning models (e.g., random forests, gradient boosting, or neural networks) may further refine prediction accuracy while uncovering nonlinear relationships among descriptors.

Bifurcation and Energetic Mapping:

A broader series of acenes, pericondensed hydrocarbons, and heteroaromatics can be analyzed to map bifurcation points more comprehensively, identifying structural thresholds that trigger energetic transitions.

Software Implementation:

Developing a dedicated computational tool or Python package for automatic computation of C(G) and visualization of descriptor trends would facilitate accessibility and reproducibility in chemical informatics research.

Acknowledgements

The authors express gratitude to the Department of Math at NCBA&E, Multan Campus, for providing computational facilities and academic support.

References

- 1. H. Wiener, H. J. Am. Chem. Soc. 69(1):17–20, (1947).
- 2. I. Gutman, Trinajstić, N. Chem. Phys. Lett. 17(4):535–538, (1972).
- 3. M. Randić, J. Am. Chem. Soc. 97(23):6609–6615, (1975).
- 4. A. E. Hoerl, Kennard, R.W. *Technometrics* 12(1):55–67, (1970).

- 5. H. Mukhtar, Saleem, M., & Nawaz, T.P. *Int. J. Res. Studies*, 5, 1–15 **(2025)**. DOI: https://doi.org/10.5281/zenodo.17290956
- 6. Estrada, E. *The Structure of Complex Networks: Theory and Applications*; Oxford University Press: Oxford, (2011).
- 7. Bonchev, D., Buck, G.A. *Complexity in Chemistry, Biology, and Ecology*; Springer: Berlin, 191–235, 191–235. (2005/2007).
- 8. Z. Gao, Z., Liu, Y., Zhang, W., & Chen, X. Computational and Theoretical Chemistry, 1201, 113223 (2021).
- 9. R. Singh, Sharma, R. J. Mol. Graph. Model. 113:108171, (2022).
- 10. A. Patel, Chauhan, S.A. Comput. Chem. Res. 5(2):99–109, (2023).
- 11. M. A. Hassan, M.A., Rehman, S., & Ali, N. Arab. J. Chem, 13(12), 8557–8573 (2020).
- 12. Ng, T.Y., Ong, C.W. J. Comput. Chem. 45(3):377–389, (2024).
- 13. H. Mukhtar, Saleem, M., Nawaz, T.P., & Farhad, K. *The Critical Review of Social Sciences Studies*, 3(4), 587–600 (2025).
- 14. D. Bonchev, Buck, G.A. Int. J. Chem. Model. 47(2):41–58, (2005).
- 15. M.Y. Diudea, M.V. *QSPR/QSAR Studies by Molecular Descriptors*; Nova Science Publishers: New York, (2000).
- 16. H. Mukhtar, M. Saleem, T. Perveen. Acad. Int. J. Soc. Sci. (AIJSS), 4 (3). 155–178 (2025).

Received: October 10th 2025 Accepted: November 2nd 2025